Journal of Molecular Structure 1086 (2015) 56–63

Contents lists available at ScienceDirect

Journal of Molecular Structure

journal homepage: www.elsevier.com/locate/molstruc

Synthesis, structural characterization, *in-vitro* antibiogram assay and efficient catalytic activities of transition metal(II) chelates incorporating (E)-(2-((2-hydroxybenzylidene)amino)phenyl)(phenyl)methanone ligand

Vellaichamy Muniyandi [a], Narayanaperumal Pravin [a], Liviu Mitu [b], Natarajan Raman [a,*]

[a] Research Department of Chemistry, VHNSN College, Virudhunagar 626 001, Tamil Nadu, India
[b] Department of Chemistry, University of Pitesti, Pitesti 110 040, Romania

HIGHLIGHTS

- Synthesis of new DNA targeting metal chelates.
- Square planar geometrical arrangements of the complexes.
- The newly synthesized metal chelates act as persistent intercalators.
- Metal chelates display better chemical nuclease activity.
- They exhibit excellent catalytic performance towards the oxidation of toluene.

GRAPHICAL ABSTRACT

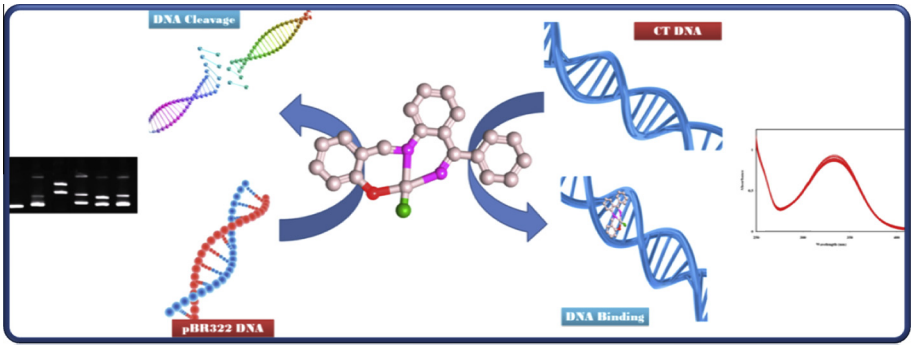

ARTICLE INFO

Article history:
Received 3 December 2014
Received in revised form 6 January 2015
Accepted 6 January 2015
Available online 13 January 2015

Keywords:
Square planar
Intercalation
Biological activity
DNA cleavage
Catalytic activity

ABSTRACT

A new tridentate ligand, (E)-(2-((2-hydroxybenzylidene)amino)phenyl)(phenyl)methanone and its four metal(II) chelates have been designed and synthesized. They were structurally characterized by elemental analysis, FT IR, UV–vis, ^{1}H NMR, ^{13}C NMR, mass spectra, EPR, magnetic moment and conductivity measurements. Elemental analysis and molar conductance values reveal that all the chelates are 1:1 stoichiometry of the type [MLCl] having non-electrolytic nature. The metal chelates adopt square planar geometrical arrangements around the metal ions. The DNA-binding properties of these chelates have been investigated by electronic absorption, cyclic voltammetry, differential pulse voltammogram and viscosity measurements. The data indicate that these complexes bind to DNA *via* an intercalation mode. The oxidative cleavage of the metal complexes with pBR322 DNA has also been investigated by gel electrophoresis. Moreover, the antimicrobial bustle shows that all metal chelates have superior activity than the free ligand. The oxidation of toluene to benzaldehyde is effectively catalyzed by the synthesized chelates.

Introduction

For the past few decades, transition metal complexes have been paid much attention in the study of mutation of genes in therapeutic approaches [1,2]. In chemotherapeutic approach DNA will be the

* Corresponding author. Tel.: +91 092451 65958; fax: +91 4562 281338.
E-mail address: ramchem1964@gmail.com (N. Raman).

http://dx.doi.org/10.1016/j.molstruc.2015.01.011
0022-2860/

target molecule in the treatment of cancer. Nowadays cis-platin and trans-platin are used as anticancer drugs. From these two drugs, cis-platin is an efficient chemotherapeutic agent for treating various types of cancers such as sarcomas, small cell lung cancer, ovarian cancer, lymphomas and germ cell tumors [3] but it encounters a number of side effects such as anaemia, diarrhea, alopecia, petechiae, fatigue nephrotoxicity, emetogenesis, ototoxicity and neurotoxicity [4]. To surmount this issue, present inorganic chemists design more effective, cheaper, less toxic, site specific, and preferably non-covalently bound anticancer drugs. A new approach in this task is to examine the anticancer activity of complexes containing transition metal ions other than platinum. Late first row transition metals *viz,* cobalt, nickel, copper and zinc are biologically relevant metals as they are associated with various biomolecules related to essential physiological activities [5]. At present, the bioactive novel Schiff base ligands containing N, O/S donor sites with transition metal complexes have considerable attention in the treatment of cancer cells in chemotherapeutic field [6–9].

Benzophenone [(2-aminophenyl)(phenyl)methanone] and its derivatives play an important role in organic chemistry, since they are intermediates in several syntheses of pharmaceuticals, such as benzodiazepines [10], diazocines [11] and in many photoreactions, including photo-Fries and the photo-Claisen rearrangements [12] which also present variable coordinating behavior toward metal ions. In particular, it has been observed that the introduction of another potential binding site such as an amino group modifies both roles of benzophenone as sensitizer [13] and its co-ordinating ability [14], suggesting a correlation between these properties. It is familiar that DNA is the hereditary material in humans and almost all other organisms. Although simple in structure, DNA can code for all the complex necessities of life [15]. Interaction of DNA with metal complexes has been investigated to design the new types of pharmaceutical architecture, the mechanism involved in the site specific recognition of DNA and to determine the principles governing the recognition [16–19].

In the light of the above and in continuation of our ongoing research on DNA binding and cleavage activities of transition metal complexes [20–22], herein we describe the synthesis and characterization of few transition metal(II) complexes containing tridentate ligand. In addition to this, DNA binding and cleavage aptitude of these complexes have been evaluated. Moreover, the catalytic activity has been explored. The antimicrobial potential of the complexes has also been probed.

Results and discussion

All the metal complexes are stable at room temperature. The free ligand is soluble in common organic solvents, but the complexes dissolve readily only in DMSO and DMF. Analytical data of the complexes suggest that the stoichiometry of the complex composition is 1:1 (*i.e.,* [MLCl]).

IR spectra

In the free ligand, the strong band observed at 1641 cm^{-1} can be assigned to the ν (—CH═N) azomethine stretching vibration. On complexation, this band was shifted to lower frequency *ca.* 1610–1618 cm^{-1} indicating the coordination of the azomethine nitrogen atom to the central metal ion. The spectrum of the ligand (Fig. S1) showed a broad band at 3431 cm^{-1}, which can be attributed to the stretching vibration of the O—H group [23]. Absence of this band in all the complexes was confirmed by the coordination of phenolic oxygen to metal ions. Moreover, the chelation was further confirmed by the formation of metal–oxygen bond in the complexes in the region 556–566 cm^{-1}. The new band observed in the complexes in the range 471–487 cm^{-1} indicates the formation of metal-nitrogen bond. From the IR results, it is concluded that the Schiff base ligand acts as tridentate (Scheme 1) and coordinates to the metal ion through carbonyl oxygen, azomethine nitrogen and phenolic oxygen atoms.

Molar conductivity

With a view to study the electrolytic nature of the mononuclear metal complexes, their molar conductivities were measured in DMF at 10^{-3} M. These values of all the complexes have been found in the range 4.1–4.9 Ω^{-1} cm^2 mol^{-1} (Table 1) indicating their non-electrolytic nature. The absence of counter (chloride) ion is confirmed from Volhard's test. Elemental analyses data suggest a 1:1 ligand to metal ratio for the complexes, and all of these data have been used to confirm the formulae of the complexes.

Electronic spectra and magnetic properties of metal(II) chelates

Electronic spectra of ligand and its metal(II) complexes were measured at room temperature in DMF solution over 200–1100 nm range. Various spectral data (Dq, B, β, β (%), ν_2/ν_1 and LFSE) for the Ni(II) and Co(II) complexes (Table 2) were calculated by applying band energies on Tanabe Sugano diagrams. The electronic absorption spectral data for ligand and its complexes were obtained in DMF solution at room temperature. The free ligand exhibited two intense bands in 32,176 and 33,487 cm^{-1} region due to $\pi \rightarrow \pi^*$ and $n \rightarrow \pi^*$ transitions, respectively. In all the metal complexes, these transitions were shifted to blue or red frequencies due to the coordination of the ligand with metal ions. The electronic spectrum of Cu(II) complex displayed the d–d transition band at 18,914 cm^{-1} (ε = 1109 L M^{-1} cm^{-1}), due to $^2B_{1g} \rightarrow {}^2A_{1g}$ transition. This d–d band strongly favors a square planar geometry around the Cu(II) ion. It is further supported by the magnetic susceptibility value (1.82 BM). The electronic spectrum of Co(II) complex showed band at 18,523 cm^{-1} (ε = 1058 L M^{-1} cm^{-1}), assigned to $^1A_{1g} \rightarrow {}^1B_{1g}$ transition which was further supported by its magnetic moment value (2.1 BM) indicating that this complex has a square planar configuration. The observed diamagnetic nature of Ni(II) complex confirmed the square planar geometry. In the zinc complex, metal to ligand charge transfer (MLCT) was also expected but it was not observed probably due to overlapping with internal electronic transitions of Schiff base ligand. Because of the d^{10} electron configuration of Zn(II), d–d electronic transitions are not observed. Hence, based on stoichiometry of this complex and elemental analysis it is four coordinated, which could be square planar geometry. Ligand field parameters such as, Racah parameter (B), β and β° values support the covalent character of the square planar geometry around Ni(II) and Co(II) complexes [24].

^1H and ^{13}C NMR spectra

^1H NMR spectrum of the (Fig. S2) ligand showed a singlet at δ 5.7, attributed to the phenolic OH group of 2-hydroxybenzaldehyde present in the ligand moiety. The absence of this peak was noted for its zinc complex confirmed the deprotonation of —OH proton with metal ion upon complexation. The aromatic region was a set of multiplets in the range of δ 6.8–7.3 for the ligand and its Zn(II) complex. The ligand also showed an azomethine proton (—CH═N) signal at δ 9.2. In complex, this signal was shifted down field (δ 8.6) suggesting deshielding of azomethine group due to the coordination with metal ion. There is no appreciable change in all other signals of the complex.

In the ^{13}C NMR spectra, the presence of a downfield shifted signal in the region 160.2 ppm with respect to that observed 158.1 ppm for the corresponding parent Schiff base (Fig. S3) was in support of coordination of azomethine nitrogen to Zn atom.

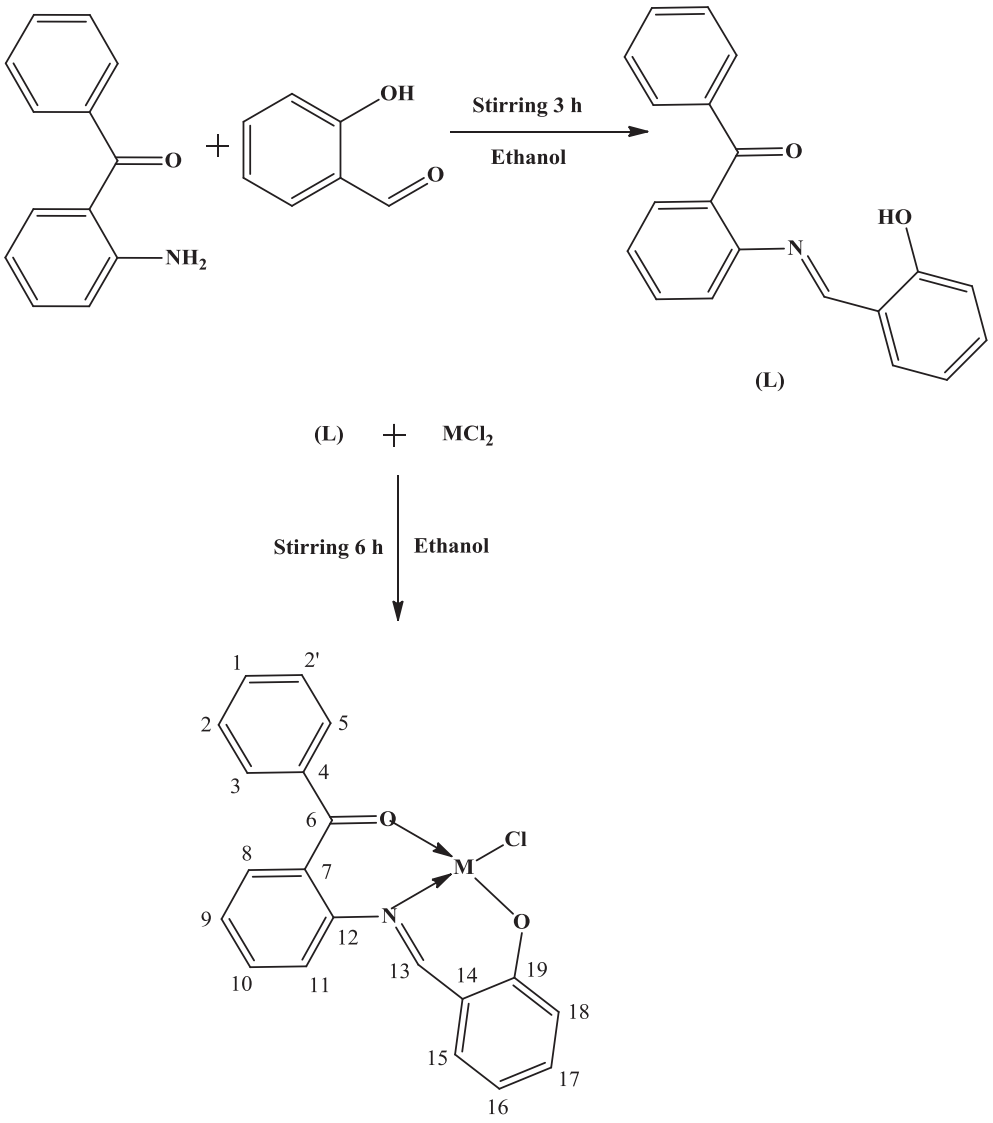

Scheme 1. Synthesis of Schiff base ligand and its metal complexes.

Table 1
Elemental and physical data of Schiff base ligand (L) and its metal(II) complexes.

Compound	Empirical formula	Formula weight	Color	Yield (%)	Elemental analysis found (Calc.)%				Λ_M (Ω^{-1} mol^{-1} cm^2)
					M	C	H	N	
[L]	$C_{20}H_{15}NO_2$	301	Pale yellow	74	–	79.6 (79.7)	4.8 (5.0)	4.6 (4.6)	–
[CuLCl]	$C_{20}H_{14}ClNO_2Cu$	399	Brown	68	15.7 (15.9)	59.9 (60.1)	3.3 (3.5)	3.4 (3.5)	4.1
[NiLCl]	$C_{20}H_{14}ClNO_2Ni$	394	Pale green	61	14.7 (14.8)	60.7 (60.9)	3.5 (3.6)	3.3 (3.5)	4.6
[CoLCl]	$C_{20}H_{14}ClNO_2Co$	394	Pale pink	65	14.7 (14.9)	60.7 (60.8)	3.4 (3.6)	3.4 (3.5)	4.7
[ZnLCl]	$C_{20}H_{14}ClNO_2Zn$	401	Yellow	68	16.1 (16.3)	59.9 (59.8)	3.4 (3.5)	3.3 (3.5)	4.9

The signal which appeared in 159.4 ppm region for the carbon atom adjacent to the phenolic oxygen in the spectrum of free ligand, has been observed in the complex at 157.1 ppm, indicating the coordination of phenolic oxygen to metal ion [25]. Comparison of all carbon peaks of the ligand with those of zinc complex showed some upfield and downfield shifts, but these shifts were not large.

Mass spectra

The mass spectrum of Schiff base ligand (Fig. S4) showed peak at *m/z* 301 corresponding to $[C_{20}H_{14}NO_2]^+$ ion. Also the spectrum exhibited peaks for the fragments at *m/z* 195, 105 and 77 corresponding to $[C_{13}H_9NO]^+$, $[C_7H_5O]^+$ and $[C_6H_5]^{+\cdot}$ respectively

Table 2
Electronic absorption spectral data (in DMF) and magnetic susceptibility of the Schiff base metal(II) complexes.

Compound	λ_{max} (cm^{-1})	Band assignments	Geometry	μ_{eff} (BM)	Ligand field parameter					
					Dq (cm^{-1})	B (cm^{-1})	β	β (%)	LFSE (kJ mol^{-1})	ν_2/ν_1
[CuLCl]	41,315	INCT	Square planar	1.82	–	–	–	–	–	–
	31,942	INCT								
	18,914	$^2B_{1g} \rightarrow {}^2A_{1g}$								
[NiLCl]	41,112	INCT	Square planar	Diamagnetic	963	903.16 (971 for free ion)	0.87	12.31	158.72	1.50
	31,214	INCT								
	20,406	$^1A_{1g} \rightarrow {}^1A_{2g}$								
	17,996	$^1A_{1g} \rightarrow {}^1B_{1g}$								
[CoLCl]	41,587	INCT	Square planar	2.1	1085	841.02 (1030 for free ion)	0.86	13.38	103.96	1.63
	31,123	INCT								
	18,523	$^1A_{1g} \rightarrow {}^1B_{1g}$								
[ZnLCl]	41,654	d–d envelope	Square planar	Diamagnetic	–	–	–	–	–	–
	31,929	LMCT ($n \rightarrow \pi^*$)								

Table 3
The spin Hamiltonian parameters of Cu(II) complex in DMSO solution at 77 K.

Complex	g-Tensor			$A \times 10^{-4}$ (cm^{-1})			f	G	α^2	β^2	$K_{\|\|}$	$K_\perp$
	$g_{\|\|}$	$g_\perp$	g_{iso}	$A_{\|\|}$	$A_\perp$	A_{iso}						
[CuLCl]	2.21	2.05	2.14	138	26	63	162	4.23	0.72	0.96	0.83	0.61

(Scheme S1, supplementary file). The mass spectrum of Cu(II) complex showed peak at *m/z* 400, corresponding to its molecular ion peak and also the isotopic peaks of all the complexes were observed with the weak relative intensities at (M + 2). In all the complexes, the observed fragment ion $[C_{20}H_{14}NO_2M]^+$ was due to the elimination of one coordinated chlorine atom. The Cu(II) complex gave a fragment ion peak with loss of one chlorine atom at *m/z* 365. All these fragments leading to the formation of the species $[ML]^+$ which further experienced de-metallation to yield the species $[L^+]$ giving the fragment ion peak at *m/z* 301.

Electron paramagnetic spectrum of the Cu(II) complex

The EPR spectrum of Cu(II) complex is very important to understand the metal ion environment in the complex [26] *i.e.,* the geometry, nature of the donating atoms from the ligand and degree of covalency of the Cu(II)-ligand bonds. The EPR spectra of the Cu(II) complex were recorded in DMSO at liquid nitrogen temperature (LNT) and at room temperature (RT). The spin Hamiltonian parameters of Cu(II) complex are listed in Table 3. The observed spectral parameters for this compound are $A_{||}$ (138) > $A_\perp$ (26); $g_{||} = 2.21$ and $g_\perp = 2.05$ and $g_{iso} = 2.14$ which indicate that the unpaired electron is localized in d^2_{xy} orbital of the Cu(II) ion with $3d^9$ configuration with considerable covalent nature [27] present in Cu-L.

The parameter G, determined as $G = (g_{||}-g_e)/(g_\perp-g_e)$, which measures the exchange interaction between the metal centers in a polycrystalline solid, has been calculated. According to Hathaway [28] if $G > 4$, the exchange interaction is negligible, but $G < 4$ indicates considerable exchange interaction in the solid complex. The Cu(II) complex gives the G value 4.23 which is greater than 4 indicating that the exchange interaction is absent in solid complex.

The observed values of α^2 and β^2 parameters indicate that the complex has some covalent character and there is interaction in the out-of-plane π-bonding. The lower value of α^2 (0.72) compared to β^2 (0.96) indicates that the in-plane σ-bonding is more covalent than the in-plane π-bonding. For the present Cu(II) complex, the observed order $K_{||}$ (0.83) was greater than $K_\perp$ (0.61) implying a greater contribution from out-of-plane π-bonding than from in-plane π-bonding in metal-ligand π-bonding. Based on these observations, a square planar geometry is proposed for Cu(II) complex. The EPR study of the Cu(II) complex has provided supportive evidence to the conclusion obtained on the basis of electronic spectrum and magnetic moment value.

DNA binding studies

Absorption spectral titrations

Electronic absorption spectroscopy is a useful technique in DNA binding studies of molecules. DNA usually exhibits hypochromism and red shift (bathochromism) as a consequence of the intercalation mode, which involves a strong stacking interaction between an aromatic chromophore and the base pairs of DNA. This strong stacking interaction is due to the contraction of calf thymus CT DNA in the helix axis and its conformational changes. On the other hand, hyperchromism results from the secondary damage of DNA double helix structure, in which the extent of hyperchromism is indicative of partial or non-intercalative binding modes [29].

The absorption spectrum of [CuLCl] in the absence and presence of CT DNA is given in Fig. 1. As the DNA concentration is increased, the MLCT transition band of [CuLCl] complex at 335 nm exhibits hypochromism of about 10% and bathochromism of 4 nm respectively, further the intense absorption bands with maxima of 336, 335 and 336 nm for [NiLCl], [CoLCl] and [ZnLCl] exhibit hypochromism of about 5%, 5%, 6% and bathochromism of 4, 3, and 3 nm, respectively. These spectral characteristics may suggest a mode of binding that involves a stacking interaction between the aromatic chromophore and the DNA base pairs. The hypochromisms observed for the bands of these four compounds are accompanied by a small red shift by less than 4 nm. The above phenomena imply that these compounds interact with CT DNA by intercalative binding mode. To compare quantitatively the affinity of these compounds binding to DNA, the intrinsic binding constant (K_b) has been estimated. From absorption data, K_b is determined using the following equation [30]:

$$[DNA]/(\varepsilon_a - \varepsilon_f) = [DNA]/(\varepsilon_b - \varepsilon_f) + [K_b(\varepsilon_b - \varepsilon_f)]^{-1}$$

where [DNA] is the concentration of DNA in base pairs, the apparent absorption coefficients ε_a, ε_f, and ε_b are the apparent, free and bound metal complex extinction coefficients, respectively. A plot of [DNA]/(ε_b–ε_f) *vs* [DNA], gives a slope of $1/(\varepsilon_b–\varepsilon_f)$ and a y-intercept equal to

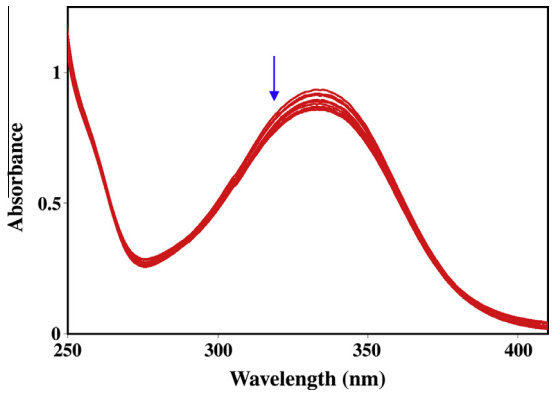

Fig. 1. Absorption spectrum of [CuLCl] in buffer pH = 7.2 at 25 °C in presence of increasing amount of DNA. The arrow indicates increasing the amount of DNA.

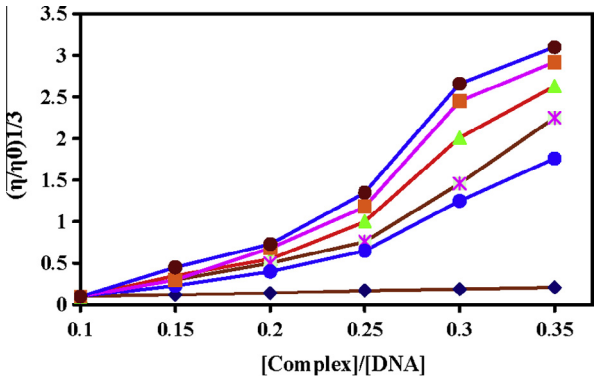

Fig. 2. Effect of increasing amount of [EB] (●), [CuLCl] (■), [CoLCl] (▲), [NiLCl] (ж), [ZnLCl] (●) and L (♦) on the viscosity of DNA. *R* = [complex]/[DNA] or [EB]/[DNA].

Table 4
Intrinsic binding constant (K_b) values of Schiff base metal(II) complexes.

Complexes	λ_{max} (nm)		$\Delta\lambda$ (nm)	%H	$K_b \times 10^4$ (M^{-1})	ΔG (KJ mol^{-1})
	Free	Bound				
[CuLCl]	331	335	4	10	1.68	−24.07
[NiLCl]	332	336	4	5	1.60	−23.96
[CoLCl]	332	335	3	5	1.66	−24.07
[ZnLCl]	333	336	3	6	1.47	−23.73

$[K_b/(\varepsilon_b-\varepsilon_f)]^{-1}$. K_b is the ratio of the slope to the y-intercept. Intrinsic binding constants of 1.68×10^4, 1.60×10^4, 1.66×10^4, 1.47×10^4 have been determined for [CuLCl], [NiLCl], [CoLCl] and [ZnLCl] respectively. The results suggest that the interaction of metal(II) complexes with DNA is a significant intercalative binding mode. The K_b values (Table 4) obtained here is lower than that reported for a few metallointercalators $[Ru(bpy)_2(dppz)]^{2+}$ (4.90×10^6 M^{-1}) [31] and $[Ru(bpy)^2(HBT)]^{2+}$ (5.71×10^7 M^{-1}) [32].

Viscosity measurements

Hydrodynamic measurements (*i.e.*, viscosity and sedimentation) that are sensitive to length changes are the most critical and least ambiguous tests of binding in solution without crystallographic data [33]. A classical intercalation model results in the lengthening of the DNA helix as the base pairs are separated to accommodate the binding molecule leading to an increase in the DNA viscosity. However, a partial and/or non-classical intercalation of ligand may bend (or kink) DNA helix, resulting in the decrease of its effective length and concomitantly its viscosity [34]. The effects of all the compounds and together with ethidium bromide [EB] on the viscosity of CT DNA are shown in Fig. 2. On increasing the amount of metal complexes, the relative viscosity of DNA moderately increased steadily, which is similar to the behavior of ethidium bromide. The results suggest that all the metal complexes bind to DNA with intercalative mode. The viscosity measurements clearly show that all the compounds can intercalate between adjacent DNA base pairs, causing an extension in the DNA helix and thus increasing the viscosity of DNA with an increasing concentration of the complexes. On the basis of all the spectroscopic studies together with the viscosity measurements, we find that the metal complexes can bind to CT DNA *via* an intercalative mode.

Electrochemical behavior

The application of electrochemical methods to the study of organic and metallointeraction to DNA provides a useful complement to the previously used methods of investigation, such as UV–vis spectroscopy and viscosity studies [35]. Small molecules, which are not amenable to such methods either because of weak absorption bands or because of overlap of electronic transition with those of the DNA molecules, can potentially, be studied *via* voltammetric techniques. Cyclic voltammogram of Cu(II) complex in the absence and presence of CT DNA is shown in Fig. 3. As seen in this figure, in the absence of CT DNA the cyclic voltammogram featured anodic peak Ep_a (−0.172 V) and cathodic peak Ep_c (−0.786 V) at 0.1 V s^{-1}. The reduction and oxidation potential observed at Ep_c = −0.767 V and Ep_a = −0.166 V is assigned to the redox couple, Cu(II)/Cu(I). The ratio of Ip_a/Ip_c peak current is 0.30 (less than unity), indicating a quasi-reversible redox process.

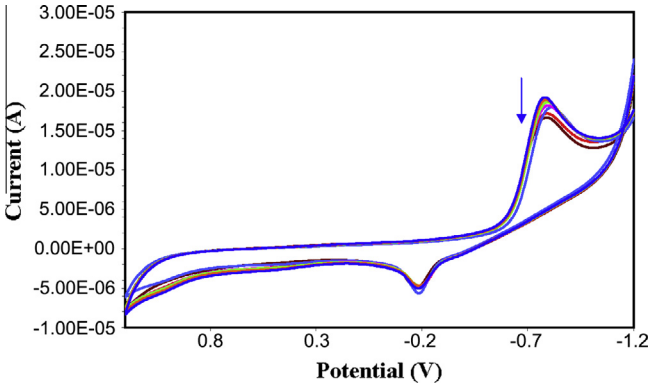

Fig. 3. Cyclic voltammogram of [CuLCl] in buffer pH = 7.2 at 25 °C in presence of increasing amount of DNA. The arrow indicates increasing the amount of DNA.

For the cyclic voltammogram of Ni(II) complex in the absence of DNA, the anodic peak Ep_a (1.021 V) and cathodic peak Ep_c (−0.671 V) appeared at 0.1 V s^{-1} for Ni(II) → Ni(I), (Ep_a = 1.101 V, Ep_c = −0.651 V, ΔEp = 1.752 V and $E_{1/2}$ = 0.225 V). The ratio of Ip_a/Ip_c peak current is 0.66, indicating a quasi-reversible redox process. The cyclic voltammogram of Co(II) complex featured anodic peak Ep_a (0.96 V) and cathodic peak Ep_c (−0.718 V) at 0.1 V s^{-1}. The reduction and oxidation potential observed at Ep_c = −0.637 V and Ep_a = 1.021 V is assigned to the redox couple Co(II)/Co(I). The ratio of Ip_a/Ip_c peak current is 0.63, indicating a quasi-reversible redox process. In Zn(II) complex, in the absence of DNA the anodic peak (0.906 V) and cathodic peak (−0.735 V) at 0.1 V s^{-1} for Zn(II) → Zn(0), (Ep_a = 1.012 V, Ep_c = −0.701 V, ΔEp = 1.713 V, and $E_{1/2}$ = 0.155 V). The ratio of Ip_a/Ip_c peak current is less than unity (0.38), indicating a quasi-reversible redox process (Table 5). The incremental addition of CT DNA to the complexes revealed that the redox couples caused a more positive shift in $E_{1/2}$ and decrease

Table 5
Electrochemical parameters for the interaction of DNA with Cu(II), Ni(II), Co(II) and Zn(II) complexes.

Compound	Redox couples	[a]$E_{1/2}$ (V)		[b]ΔEp (V)		Ip_a/Ip_c
		Free	Bound	Free	Bound	
[CuLCl]	Cu(II) → Cu(I)	−0.479	−0.466	0.614	0.601	0.30
[NiLCl]	Ni(II) → Ni(I)	0.164	0.225	1.67	1.752	0.66
[CoLCl]	Co(II) → Co(I)	0.121	0.192	1.678	0.384	0.63
[ZnLCl]	Zn(II) → Zn(0)	0.085	0.155	1.641	1.713	0.38

Data from cyclic voltammetric measurements.
[a] $E_{1/2}$ is calculated as the average of anodic (E_{Pa}) and cathodic (Ep_c) peak potential; $^aE_{1/2} = (Ep_a + Ep_c)/2$.
[b] $\Delta Ep = Ep_a - Ep_c$.

of ΔEp. The Ip_a/Ip_c values also decreased in the presence of DNA. Bard has reported [36] that if $E_{1/2}$ is shifted to more positive value, the interaction mode is intercalative binding. The above results of metal-DNA interaction by the cyclic voltammogram studies confirm that Cu(II), Ni(II), Co(II) and Zn(II) complexes bind to DNA *via* intercalation binding mode.

Differential pulse voltammogram of the Cu(II) complex in the absence and presence of varying concentration of DNA is shown in Fig. 4. Increase in concentration of DNA causes a negative potential shift along with significant decrease of current intensity. The shift in potential is related to the ratio of binding constant:

$$E_b^0 - E_f^0 = 0.0591 \log(K_+/K_{2+})$$

where $E^0{}_b$ and $E^0{}_f$ are formal potentials of the Cu(II), Ni(II), Co(II) and Zn(II) complex couples in the bound and free form respectively. In the present study, all the complexes exhibited one electron transfer during the redox process. The ratio of the binding constants ($K_{[red]}/K_{[oxd]}$) for DNA binding of synthesized complexes was calculated and found to approximately less than unity. The above electrochemical experimental results indicate the preferential stabilization of Cu(II), Ni(II), Co(II) and Zn(II) forms over other forms on binding to DNA. In this study, the synthesized complexes reveal that both anodic and cathodic peak potential shifts are either positive or negative. In this regard, the present Cu(II) complex shows a positive potential shift along with significant decreasing of current intensity during the addition of increasing amount of DNA. It indicates that copper ion stabilizes the duplex (GC pairs) by intercalating way.

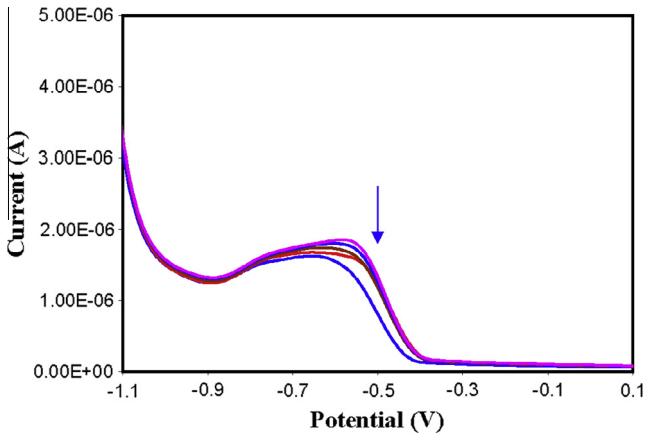

Fig. 4. Differential pulse voltammogram of [CuLCl] in buffer pH = 7.2 at 25 °C in presence of increasing amount of DNA. The arrow indicates increasing the amount of DNA.

DNA cleavage efficacy

There are number of agents which exert their effect by inhibiting enzymes that act upon DNA. These inhibitions result from the binding of such agents to the enzyme site of interaction on the DNA rather than to direct enzyme inactivation. Transition metals have been reported to inhibit DNA repair enzymes. The DNA cleavage efficiency of complex is attributed to the different binding affinity of complex to DNA. There has been considerable interest in DNA cleavage reactions activated by transition metal complexes. The delivery of metal ion to the helix, in locally generating oxygen or hydroxide radicals, yields an efficient cleavage reaction [37]. Gel electrophoresis is a technique based on the migration of DNA under the influence of an electric potential. When the original supercoiled form (Form I) of plasmid DNA is nicked an open circular relaxed form (Form II) will exist in the system and the linear form (Form III) can be found upon further cleavage. When circular plasmid DNA is run on horizontal gel by electrophoresis, the compact Form I migrates relatively faster while the nicked Form II migrates slowly, and the linearized Form III migrates between Forms I and II.

To assess the DNA cleavage ability of our synthesized metal(II) complexes, supercoiled (SC) pBR322 DNA was incubated with the complexes in 5 mM Tris-HCl/50 mM NaCl buffer at pH 7.2 for 2 h. The cleavage experiments were carried out in the presence of activating agent, H_2O_2 under aerobic conditions and are shown in Fig. 5. The intensity of supercoiled SC (Form I) diminished gradually and completely converted to nicked form (NC) (Form II). The intensity of the NC (Form II) band increased whereas the production of linear form L (Form III) of DNA also increased in the presence of H_2O_2 [38]. Control experiments have suggested that untreated DNA did not show any cleavage (lane 1). Moreover, uncoordinated ligand did not show any apparent cleavage (lane 2). These experimental facts demonstrate that a combination of all the metal(II) complexes and activating agent (H_2O_2) are required to show effective cleavage of plasmid DNA. It is obvious that Cu(II) (Fig. 5; lane 4) has more ability to cleave the supercoiled plasmid DNA when compared to that of other complexes. It is believed that the cleavage ability of complexes is due to the reaction of metal ions with H_2O_2 which produces diffusible hydroxyl radicals or molecular oxygen at ease which in turn damage DNA through Fenton-type chemistry [39].

Antimicrobial activity

The biological activities of the Schiff base ligand (L) and its metal(II) complexes were tested against few bacteria and fungi. All of the tested compounds showed a remarkable biological activity against different types of Gram-positive and Gram-negative bacteria and against fungi species. The minimal inhibitory concentrations of tested compounds against certain bacteria and fungi are

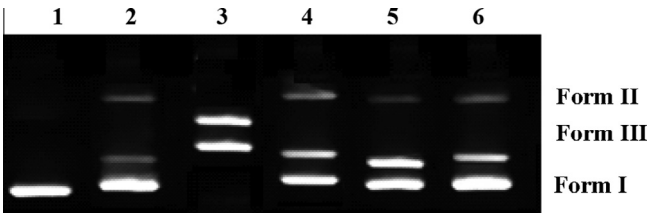

Fig. 5. Gel electrophoresis pattern showing cleavage of pBR322 supercoiled DNA (10 μM) by Cu(II), Ni(II), Co(II) and Zn(II) complexes (60 μM) in the presence of H_2O_2 (100 μM). Lane 1: DNA alone; lane 2: DNA + [L] + H_2O_2; lane 3: [CuLCl] + DNA + H_2O_2; lane 4: [CoLCl] + DNA + H_2O_2; lane 5: [NiLCl] + DNA + H_2O_2; lane 6: [ZnLCl] + DNA + H_2O_2.

Table 6
Minimum inhibitory concentration of the synthesized compounds against the growth of bacteria (μM).

Compound	Minimum inhibitory concentration (MIC) ($\times 10^4$ μM)				
	S. aureus	*P. aeruginosa*	*E. coli*	*S. epidermidis*	*K. pneumoniae*
[L]	16.9	15.8	16.4	16.2	14.5
[CuLCl]	7.1	8.1	6.2	7.7	7.3
[NiLCl]	9.4	9.6	9.0	9.7	9.2
[CoLCl]	8.4	7.1	8.6	6.3	7.9
[ZnLCl]	11.3	10.8	13.5	12.1	11.7
[a]Streptomycin	1.7	1.9	1.8	1.3	2.3

[a] Streptomycin is used as the standard.

Table 7
Minimum inhibitory concentration of the synthesized compounds against the growth of fungi (μM).

Compound	Minimum inhibitory concentration (MIC) ($\times 10^4$ μM)				
	A. niger	*F. solani*	*C. lunata*	*R. bataticola*	*C. albicans*
[L]	13.9	19.3	16.5	11.9	14.9
[CuLCl]	9.3	9.8	13.7	10.1	11.6
[NiLCl]	10.2	10.9	13.5	11.7	10.9
[CoLCl]	9.9	10.2	12.9	10.3	11.8
[ZnLCl]	12.3	12.3	12.1	12.9	11.3
[a]Nystatin	1.1	1.6	1.2	1.0	1.5

[a] Nystatin is used as the standard.

shown in Tables 6 and 7. The remarkable activity of the Schiff base ligand may be arise from the hydroxyl group which may play an important role in the antibacterial activity, as well as the presence of one azomethine group which imports in elucidating the mechanism of transformation reaction in biological systems. The obtained results indicate that the complexes have higher activity than the ligand against the same microorganisms under identical experimental conditions. This suggests that the chelation could facilitate the ability of a complex to cross a cell membrane and can be explained by Tweedy's chelation theory [40]. Chelation considerably reduces the polarity of the metal ion because of partial sharing of its positive charge with donor groups and possible electron delocalization over the whole chelate ring. Such a chelation could enhance the lipophilic character of the central metal atom, which subsequently favors its permeation through the lipid layer of the cell membrane.

Catalytic activity

The catalytic oxidation of toluene under aerobic conditions is significantly a fascinating reaction, because the direct functionalisation of inactivated —C—H bonds in hydrocarbons usually requires drastic reaction conditions such as high temperature and pressure. Fig. 6 shows the oxidation of toluene into benzaldehyde. The peak at 350 nm is the characteristic peak for the benzaldehyde [41]. The conversion percentage of toluene at room temperature and 70 °C is 0 and 68 respectively (Scheme 2). There is no product obtained at room temperature. It is noted that temperature has a significant effect on the efficiency of present catalytic system [42]. The results also explore that no oxidation takes place without the catalyst. According to the results obtained from the UV analyses, the peak may be the oxidation of toluene to benzaldehyde. Copper complex is the most efficient catalyst with the 68% conversion of toluene. Other three complexes have considerably low conversion percentages only at 70 °C *viz.*, 58%, 64% and 65% respectively (Table 8). Very important point in the oxidation of toluene is the reduction of M(II) to M(I) of the complexes. This

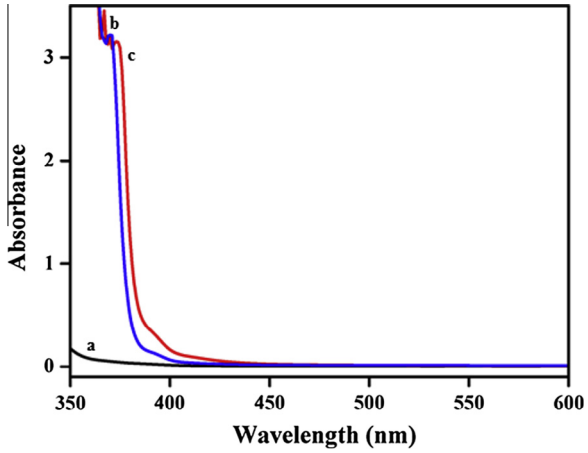

Fig. 6. The catalytic behavior of Cu(II) complex. (a) Absorption peak of toluene without Cu(II) complex, (b) reaction in the presence of Cu(II) complex at 70 °C (5 h) and (c) reaction in the presence of Cu(II) complex at 70 °C (6 h).

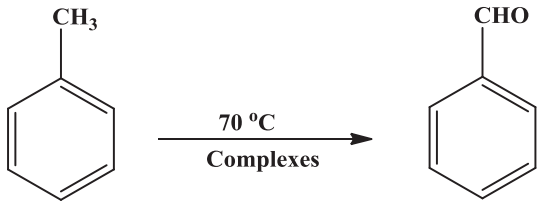

Scheme 2. The catalytic activity of Cu(II), Ni(II), Co(II) and Zn(II) Schiff base complexes in the conversion of toluene to benzaldehyde.

Table 8
Catalytic efficiency of Cu(II), Ni(II), Co(II) and Zn(II) complexes.

Compound	[CuLCl]	[NiLCl]	[CoLCl]	[ZnLCl]
@ 70 °C	68	58	64	65
@ Room temperature with catalyst	NR	NR	NR	NR
@ 70 °C without catalyst	NR	NR	NR	NR

NR – No Reaction.

reduction of M(II) facilitates the ligand around the metal ion. This catalytic system does not require any oxidant to carry out the reaction. Hence, this is an efficient and environmental friendly catalyst.

Conclusion

Few metal(II) chelates have been synthesized from 2-aminobenzophenone analogue. The physico-chemical and spectral data reveal that all the metal chelates are mononuclear and adopted square planar geometry around the metal ions. The results of DNA binding studies suggest that the complexes bind with CT DNA through intercalation mode. The agarose gel electrophoresis studies show that the complexes can promote the oxidative cleavage of plasmid DNA. However, these observations and a more extensive study would be necessary in order to assert that the complexes act as cleavage agents. All the metal chelates show considerable catalytic efficiency towards the oxidation of toluene. Cu(II) complex exhibits the highest activity as compared with other three complexes. Moreover, the compounds show antimicrobial activity against selected kinds of bacteria and fungi. The results of this antimicrobial work can show that the approach of coordinating 2-aminobenzophenone analogues with pharmacologically interesting metals such as copper, nickel and zinc could be a

suitable strategy to develop novel therapeutic tools for the medical treatment.

Acknowledgements

The authors express their sincere thanks to the College Managing Board, Principal and Head of the Department of Chemistry, VHNSN College, Virudhunagar, India for providing necessary research facilities.

Appendix A. Supplementary material

Supplementary data associated with this article can be found, in the online version, at http://dx.doi.org/10.1016/j.molstruc.2015.01.011.

References

[1] B. Selvakumar, V. Rajendiran, P.U. Maheswari, H. Stoeckli -Evans, M. Palaniandavar, J. Inorg. Biochem. 100 (2006) 316–330.
[2] M. Yodoshi, M. Odoka, N. Okabe, Chem. Pharm. Bull. 55 (2007) 853–860.
[3] E.R. Jamieson, S.J. Lippard, Chem. Rev. 99 (1999) 2467–2498.
[4] Sweetman, Sean, Martindale: The Complete Drug Reference, 37th ed., Pharmaceutical Press, 2011.
[5] P.P. Netalkar Sandeep, P.N. Srinivasa Budagumpi, V.K. Revankar, Eur. J. Med. Chem. 79 (2014) 47–56.
[6] N. Raman, R. Jeyamurugan, R. Senthilkumar, B. Rajkapoor, S.G. Franzblau, Eur. J. Med. Chem. 45 (11) (2010) 5438–5451.
[7] M.H. Habibi, E. Shojaee, M. Ranjbar, H.R. Memarian, A. Kanayama, T. Suzuki, Spectrochim. Acta 105A (2013) 563–568.
[8] M.H. Habibi, E. Askari, Synth. React. Inorg. Met.-Org. Nano-Met. Chem. 43 (2013) 400–405.
[9] M.H. Habibi, E. Askari, Synth. React. Inorg. Met.-Org. Nano-Met. Chem. 43 (2013) 406–411.
[10] E. Testa, L. Fontanella, M. Bovara, Furmuco (Puuiu), Ed. Sci. 18 (1963) 815–823.
[11] D.M. Wakankar, B.D. Hosangadi, Indian J. Chem., Sect. B 19 (1980) 703–704.
[12] M.L.M. Schilling, J. Am. Chem. Soc. 103 (1981) 3077–3081.
[13] G. Favaro, F. Masetti, J. Photochem. 15 (1981) 241–254.
[14] I.M. Vezzosi, A. Albinati, F. Ganazzoli, Inorg. Chim. Acta 96 (1984) 9–13.
[15] C.R. Calladine, H.R. Drew, B.F. Luisi, A.A. Travers, Understanding DNA: The Molecule and How it Works, 3rd ed., Elservier Ltd., 2004.
[16] R.S. Kumar, S. Arunachalam, V.S. Periasamy, C.P. Preethy, A. Riyasdeen, M.A. Akbarsha, Eur. J. Med. Chem. 43 (2008) 2082–2091.
[17] M. Yodoshi, M. Odoko, N. Okabe, Chem. Pharm. Bull. 55 (2007) 853–860.
[18] K. Jiao, Q.X. Wang, W. Sun, F.F. Jian, J. Inorg. Biochem. 99 (2005) 1369–1375.
[19] H. Yin, H. Liu, M. Hong, J. Organomet. Chem. 713 (2012) 11–19.
[20] N. Raman, K. Pothiraj, T. Baskaran, J. Mol. Struct. 1000 (2011) 135–144.
[21] N. Raman, M. Selvaganapathy, R. Senthilkumar, Inorg. Chem. Commun. 39 (2014) 99–105.
[22] N. Raman, N. Pravin, Eur. J. Med. Chem. 80 (2014) 57–70.
[23] K. Nakamoto, Infrared and Raman Spectra of Inorganic and Coordination Compounds, 3rd ed., John Wiley & Sons, New York, 1986.
[24] B.N. Figgs, Introduction to Ligand Field, Wiley, New York, 1966.
[25] N.A. Oztas, G. Yenisehirli, N. Ancin, S.G. Oztas, Y. Ozcan, S. Ide, Spectrochim. Acta, Part A 72 (2009) 929–935.
[26] A.S. El-Tabl, M.M.E. Shakdofa, A.M.A. El-Seidy, J. Chem. Soc. 55 (2011) 603–611.
[27] D. Kivelson, R. Neiman, J. Chem. Phys. 35 (1961) 149–155.
[28] B.J. Hathaway, J.N. Bardley, R.D. Gillard (Eds.), Essays in Chemistry, Academic Press, New York, NY, USA, 1971.
[29] S. Rajalakshmi, T. Weyhermüller, A.J. Freddy, H.R. Vasanthi, B.U. Nair, Eur. J. Med. Chem. 46 (2011) 608–617.
[30] A. Wolfe, G.H. Shimer, T. Meehan, Biochemistry 26 (1987) 6392–6396.
[31] S.R. Smith, G.A. Neyhart, W.A. Karlsbeck, H.H. Thorp, New J. Chem. 18 (1994) 397–406.
[32] D.L. Arockiasamy, S. Radhika, R. Parthasarathi, B.U. Nair, Eur. J. Med. Chem. 44 (2009) 2044–2051.
[33] S. Sathyanarayana, J.C. Dabroniak, J.B. Chaires, Biochemistry 31 (1992) 9319–9324.
[34] S. Satyanarayana, J.C. Dabrowiak, J.B. Chaires, Biochemistry 32 (1993) 2573–2584.
[35] S. Mahadevan, M. Palaniandavar, Bioconjugate Chem. 7 (1996) 138–143.
[36] M.T. Carter, M. Rodriguez, A.J. Bard, J. Am. Chem. Soc. 111 (1989) 8901–8911.
[37] G. Prativel, M. Pitie, J. Benadou, B. Meunier, Angew. Chem. Int. Ed. Eng. 30 (1991) 702–704.
[38] E. Gao, Y. Sun, Q. Liu, L. Duan, J. Coord. Chem. 59 (2006) 1295–1300.
[39] P. Krishnamoorthy, P. Sathyadevi, R.R. Butorac, A.H. Cowley, N.S.P. Bhuvanesh, N. Dharmaraj, Dalton Trans. 41 (2012) 4423–4436.
[40] Y. Anjaneyulu, R.P. Rao, Synth. React. Inorg. -Org. Chem. 16 (1986) 257–272.
[41] P. Roy, M. Manassero, Dalton Trans. 39 (2010) 1539–1545.
[42] M. Hoshino, R. Konishi, N. Tezuka, I. Ueno, H. Seki, J. Phys. Chem. 100 (1996) 13569–13574.